HEAT TRANSFER AROUND A 180 DEG TURN IN A SQUARE CHANNEL

G. M. Carlomagno, G. Cardone, T. Astarita

Università di Napoli *Federico II,* DETEC
P.le Tecchio, 80 - 80125 Naples, ITALY

Abstract

The aim of the present study is to obtain detailed measurements of the convective heat transfer coefficient nearby a 180deg sharp turn in a square channel. A square two-pass channel, which is 80*mm* wide, is tested. To perform surface flow visualization and heat transfer measurements, the heated-thin-foil technique is used and results in terms of temperature maps and Nusselt number *Nu* distributions are obtained. *Nu* is computed by means of the local bulk temperature which is evaluated by making a one-dimensional energy balance along the channel. Reynolds number, based on average inlet velocity and hydraulic diameter of the channel, is varied between $1.6x10^4$ and $5.5x10^4$. By moving in the streamwise direction, at the beginning of the heated zone a rapid increase of the wall temperature is found due to the development of the thermal boundary layer. Two well distinguishable separation zones are found, one at the first outer corner of the channel and the other at the second outer corner. A third weak recirculation zone seems to appear attached to the partition wall and just downstream of its tip.

Introduction

The thermal efficiency of gas turbine engines strongly depends on the gas entry temperature; the higher this temperature, the more efficient is the turbine thermal cycle. Present advanced gas turbines operate at gas entry temperatures much higher than metal creeping temperatures and therefore require intensive cooling of their blades especially in the first stage. A way of cooling turbine blades is by means of internal forced convection: generally, cooling air from the compressor is supplied through the hub section into the blade interior and, after flowing through a serpentine passage, is discharged at the blade trailing edge. The serpentine passage is mostly made of several adjacent straight ducts, spanwise aligned, which are connected by 180deg turns. The presence of these turns causes high variations in the convective heat transfer rates with consequent increased thermal stresses in the blade wall. It has to be pointed out that the thermal load enforced by the gas stream is mainly limited to the blade external walls (side walls) and therefore the partitions between ducts may be considered as approximately adiabatic.

Several works, both experimental and numerical, deal with heat transfer aspects in rectangular channels with, more or less sharp, 180deg turns and with, or without, roughening ribs at the wall. Metzger and co-workers[1,2] report a number of researches on regionally-averaged heat transfer measurements for flow through rectangular channels with sharp 180deg turns. Chyu[3] also presents regionally-averaged heat transfer coefficients in two-pass and three-pass square channels measured by means of naphthalene sublimation. More detailed analyses, published by Han et al.[4] and Chandra et al.[5] report local heat transfer distributions along discrete lines, on smooth and rib-roughened walls, also obtained by means of the naphthalene sublimation technique. Wang and Chyu[6] numerically solved the three-dimensional transport equations and studied, for a given Reynolds number, the influence of the turning configuration on the convective heat transfer coefficient in a square duct with a 180deg turn.

Two investigations, where the temperature is measured by means of thermochromic liquid crystals, have been published. The first one, carried out by Arts et al.[7], reports on Nusselt number *Nu* distributions in a rectangular two-pass channel having an aspect ratio (width to height ratio) equal to 2 and sharp 180deg turns. The second investigation, reported by Lau et al.[8], presents local heat transfer coefficients in four-pass channels, with ducts of different aspect ratios. These works present a detailed description of the heat transfer distribution around a 180deg turn. However, Arts et al.[7] do not specify any heating in the area underneath the partition wall, whereas Lau et al.[8] mention explicitly that this area is heated in their experiments. This causes overheating of the zone close to the partition wall which in turn produces a non-symmetric *Nu* distribution in the first and the fourth straight channels, even far away from the turns. Besides, even if the conduction losses perpendicular to the measuring surface are considered in the two papers, since the

models used in both tests have relatively thick walls as compared to the channel width, tangential (along the wall) thermal conduction may significantly affect the real temperature distribution on the channel walls. Finally, in both experiments the electrical power input had to be varied to account for the limited range of liquid crystals with consequent variations of the local bulk temperature.

Detailed measurements in a 180deg turn of a channel, having an aspect ratio equal to 5 (i.e. a quasi-two dimensional flow) and heated from one side only, are presented by Astarita et al.[9] who show the presence of two well distinguishable separation zones, one at the first ou-ter corner of the channel and the other one attached to the partition wall and just downstream of its tip. The development of these separation zones is shown in ref.(10) by surface flow visualizations performed in the vicinity of a 180deg turn for aspect ratios of the channel increasing from 1 to 5. It is pointed out that, for increasing aspect ratio, first a recirculation zone appears in the first outer corner of the channel and then a separation zone occurs down-stream of the second inner corner, i.e. downstream of the tip of the partition wall and attached to this latter. Local heat transfer measurements near a sharp 180deg turn of a square channel with a transient liquid crystal technique are presented by Ekkad and Han[11] who find that the Nusselt number is much higher in the region immediately downstream of the turn.

The objective of the present work is to measure heat transfer distributions for this particular flow pattern by means of an Infrared Scanning Radiometer (IRSR) whose application to these problems is advantageous on account of its relatively good spatial resolution and thermal sensitivity. Moreover, the use of IRSR matches both qualitative and quantitative requirements. Finally, it has to be stressed that the need to produce detailed and reliable heat transfer distributions is not only important *per se* but it is also very relevant to validate computer programs which are often used to study these complex flows.

The essential features of the radiometer are: it is non-intrusive; it allows a complete two-dimensional mapping of the surface to be tested; the video signal output may be treated by digital image processing. Since the sensitivity of the infrared system is not sufficient to measure the aerodynamic heating , it is necessary to create an artificial temperature difference between the testing surface and the flow. For this reason, the model is manufactured so as to generate, by Joule effect, a constant heat flux on the measured surface.

Experimental apparatus

To study the first type of flow, an open air driven flow channel is used, which consists of two adjacent straight ducts connected by a 180deg turn, as schematically shown in *Fig. 1*. The channel cross section is square with a 80*mm* side and each duct is 2000*mm* long. These dimensions ensure a fully developed flow ahead of the 180deg turn. Tolerances are of the order of ± 0.5*mm* on channel width and ± 0.2*mm* on channel height. The central partition wall, which divides the two adjacent ducts, is 16*mm* thick and the distance of its tip from the short side of the channel is equal to 80*mm*.

From the channel the air is sucked, through a laminar mass flow meter, by a centrifugal blower which is powered by means of a variable speed electric motor. Two Pt100 RTD's measure the temperature at the entrance T_1 and the temperature at the outlet T_2 of the channel so as to monitor the overall increase of the air temperature.

The channel walls are manufactured from 20*mm* thick soft wood (to have a low thermal conductivity) but, for a length of about 1200*mm*, each of the two side walls of the channel is made of three printed circuit boards, joined together and connected in series, each one 400*mm* long. The printed circuits are designed so as to achieve a constant heat flux over the surface (except beneath the partition wall) by Joule effect and, therefore, the thickness and width of their conducting

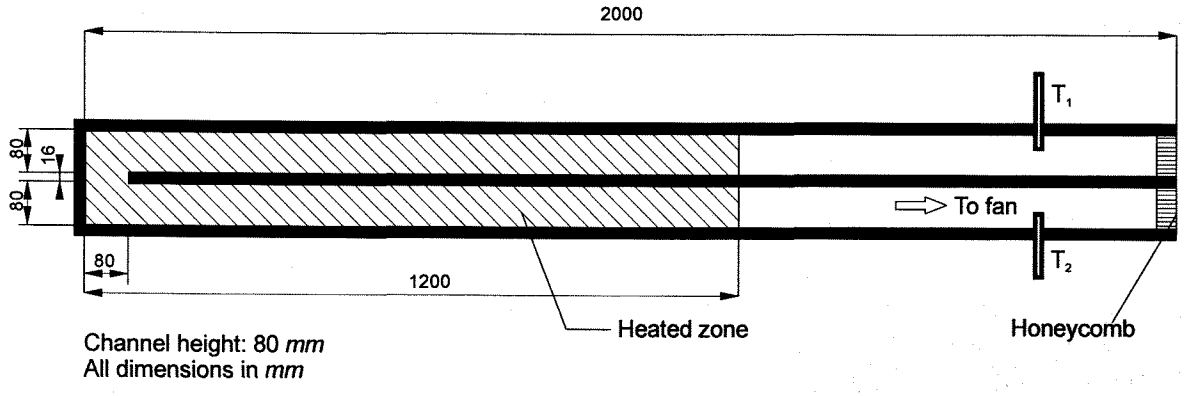

FIGURE 1 - Experimental apparatus for the 180deg turn

tracks are manufactured with very close tolerances. The tracks are 17.5μm thick, 3mm wide, placed at 3.2mm pitch and aligned with the axes of the ducts; the overall thickness of the board is 0.53mm. A stabilised DC power source supplies the electric current to the circuit and the power input is monitored by precisely measuring voltage drop and current across the circuit. Air flowing in the channel can be heated from only one of the side walls or from both of them. In the case of heating from both side walls, measurements are performed on only one of them.

Experimental procedure and data reduction

The infrared camera measures the temperature map of the model wall which is correlated to the heat transfer coefficient by means of the steady state *heated-thin-foil* technique[12]. In particular, for each pixel of the digitized thermal image, the convective heat transfer coefficient h is calculated as:

$$h = (q_w - q_r - q_c) / (T_w - T_b) \qquad (1)$$

where q_w is the Joule heat flux, q_r and q_c are the losses due to radiative flux and to tangential conduction flux respectively, T_w and T_b are the wall temperature and the local bulk temperature, respectively. Because of the low value of the pertinent Biot number, the heated wall may be considered isothermal across its thickness.

Because *heated-thin-foil* technique is implemented by means of a printed circuit board, the thermal behaviour of the foil may be non isotropic. In fact, if the circuit is obtained with several electrical conducting copper tracks arranged in a greek fret mode, the thermal conductance along the copper tracks will be much higher than in the direction perpendicular to them. Therefore, q_c is calculated from the following relationship:

$$q_c = k_x \frac{\partial^2 T}{\partial x^2} + k_y \frac{\partial^2 T}{\partial y^2} \qquad (2)$$

where k_x are k_y are thermal conductances choosed in order to take in account the shape of the printed circuit board.

The radiative thermal losses q_r are computed from the measured T_w while those due to natural convection are neglected. The local bulk temperature T_b is evaluated by measuring the stagnation temperature T_1 at the channel entrance and by making a one-dimensional energy balance along the channel, i.e. along the channel main axis; triangular heating sections are considered in the turning zone. In the latter case, by measuring T_1, T_2 and the air mass flow rate for each test run, an overall energy balance is also performed so as to compare the energy received by the fluid with the net electric power input.

The heat transfer coefficients are computed in non-dimensional form by means of the local Nusselt number:

$$Nu = h D / \lambda \qquad (3)$$

where D is the hydraulic diameter of the channel and λ the thermal conductivity coefficient of air evaluated at film temperature.

Tests are carried out for different Reynolds number Re which is defined in the conventional way:

$$Re = V D / \nu \qquad (4)$$

where V and ν are the average inlet velocity in the channel, or the free stream velocity in the tunnel test section, and the kinematic viscosity coefficient of air, respectively.

The infrared thermographic system employed is the AGEMA Thermovision 900. The field of view (which depends on the optics focal length and on the viewing distance) is scanned by the Hg-Cd-Te detector in the 8-12μm infrared window. Nominal sensitivity, expressed in terms of noise equivalent temperature difference, is 0.07°C when the scanned object is at ambient temperature. The scanner spatial resolution is 235 instantaneous fields of view per line at 50% slit response function. Each image is digitised in a frame of 136 x 272 pixels at 12 bit. Application software can be performed on each thermal image involving noise reduction by numerical filtering, computation of temperature and heat transfer correlation's.

Experimental results

The efficacy of thermography to perform this type of measurement is demonstrated by the thermogram of *Fig. 2* which shows the temperature map of the heated wall of the channel for the following testing conditions: T_1 =23.1°C, q_w =890 W/m^2, Re = 16 200, heating from one side only. As the scale on the right side of the thermogram shows, each grey level represents a

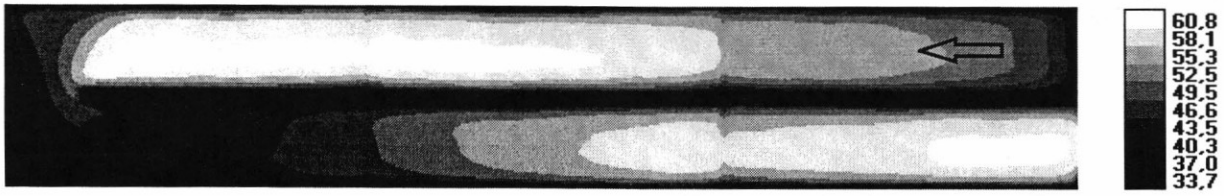

FIGURE 2 - Thermogram of the heated wall of the channel (heating from one side only)

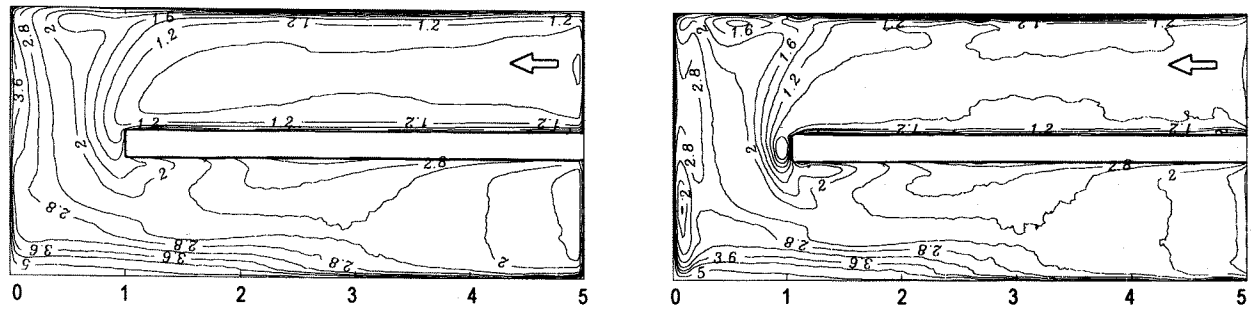

FIGURE 3 - Nusselt number maps on a 180deg turn side wall for Re = 29 000.

temperature band. White and black zones indicate temperatures above 60.8°C and below 33.7°C, respectively. It has to be pointed out that, apart from the thermal losses and the continuous increase of the bulk temperature T_b along the channel (which, in the present tests, is of the order of a few degrees Celsius), since the heat flux is practically constant over the surface, the higher the wall temperature T_w, the lower the convective heat transfer h coefficient and viceversa. Furthermore, it has to be stressed that temperature data in the neighbourhood of walls is not reliable since the latter, which are bonded to the printed circuit board and are not heated, tend to behave like fins in a stream and, therefore, produce a wall temperature decrease in their vicinity, owing to some thermal conduction within the board.

In order to gain a higher spatial resolution, the temperature map of *Fig. 2* is obtained by patching up three different thermal images acquired for the same testing conditions; the joining lines between the three boards are visible. In fact, iso-temperature contours are discontinuous at the junction lines between printed

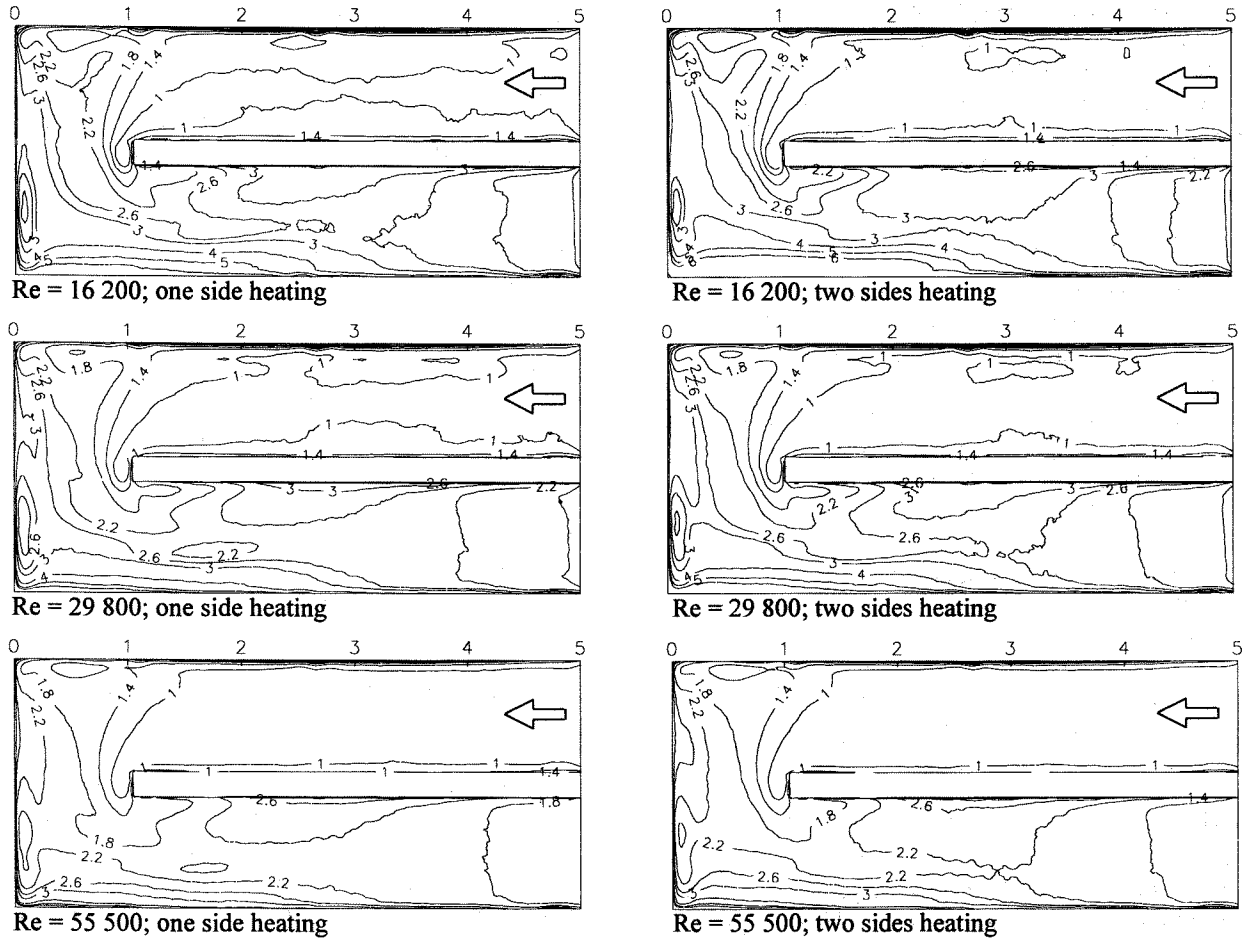

FIGURE 4 - Distribution of the local Nusselt number normalized by the value for fully developed flow

circuits in regions where the temperature is relatively constant. This is because of the high sensitivity of the infrared camera, of the turning of the tracks at the end of each printed circuit (tracks are arranged with a narrow fret shape) and mainly because of a slightly lower wall heat flux in the circuit on the right that occurs because this circuit has an electric resistance 8% lower than that of the other two boards. This is the reason why this lower resistance circuit is located at the inlet and outlet.

By moving streamwise along the channel, the quasi-regular trend of the temperature distribution across the first duct, at the beginning of the heated zone, proves a regular behaviour of the flow there. The rapid increase of wall temperature in this part of the channel accounts for the developing thermal boundary layer which, of course, starts at the starting of the heated zone. A high heat transfer region is observed just downstream of the second outer corner of the outer wall - it is due to the "jet" effect of the flow through the bend. This effect is also observed by previous authors[3,7]. Ahead of the end of the channel a completely redeveloped flow is practically recovered

The influence of tangential conduction effects are investigated in *Fig.* 3 where the distribution of the local Nusselt is presented for *Re=29 000*: the map on the left refers to data not corrected for tangential conduction (*a*) while the map on the right takes it into account. Number (*b*). The Nusselt number *Nu is* normalized by its fully developed counterpart Nu^* in a straight duct without turn, i.e. the Dittus-Boelter correlation :

$$Nu^* = 0.23\, Pr^{0.4}\, Re^{0.8} \qquad (5)$$

(*Pr* represents the Prandtl number).

As it is possible to notice, strong differences between the two maps exist in the regions where large temperature gradients are present; e.g. the recirculation zone downstream of the square tip of the partition wall, which is practically absent in the unrestored map, is well evident in the restored one.

In *Fig. 4* are shown the normalised Nusselt maps for three different Reynolds numbers. The maps on the left side are relative to heating from one side wall only while those on the right side refer to heating from both side walls.

The general trend in all maps is a Nusselt number, ahead of the turn, which practically coincides with Nu^*. Across the turn a large increase in *Nu* occurs followed by a subsequent progressive decrease further downstream. Some very high heat transfer coefficient regions are present at the wall; the first one is located on the end wall practically in front of the duct which enters the turn slightly moved towards the partition wall axis; the second region, which exhibits the highest values of Nusselt number is just downstream of the second outer

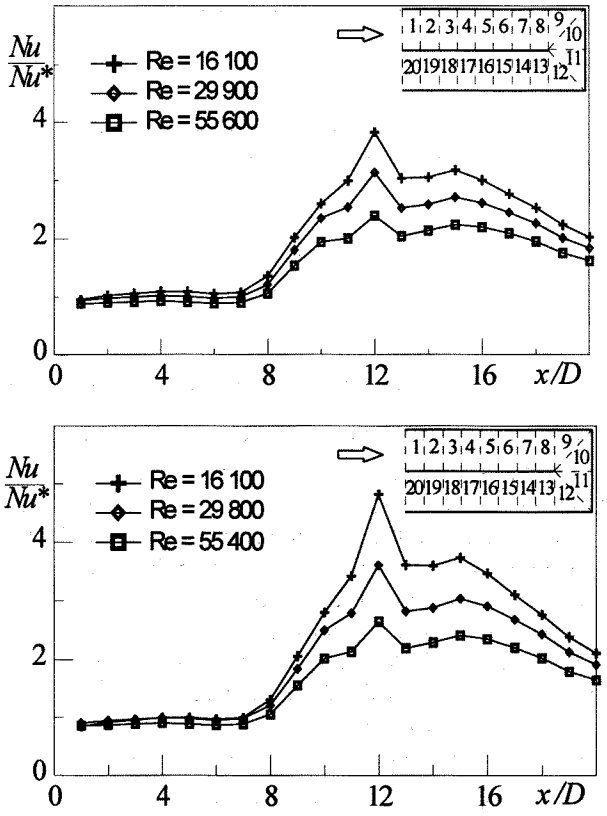

FIGURE 5 - Streamwise resolved average Nusselt number (up: heating from one side only; down: heating from both sides)

corner ; the last one is near the partition wall about two diameters downstream of the second inner corner.

Just before the first and second outer corners and attached to the external wall, two recirculation zones appear at the centre of which the Nusselt number attains a local minimum; but this minimum is always much higher than the corresponding value of Nu^*. Another region of lower *Nu* is attached to the tip of the partition wall, slipping downstream, but *Nu* values are also in this case higher than the corresponding Nu^* ones. These two findings are much different from those found by Astarita et al.[9], who measured Nusselt numbers much lower than Nu^* in these two regions for a channel of aspect ratio equal to 5.

The present Nusselt number maps look very much different from the ones computed by Wang and Chyu[6], for a different Reynolds number and thickness of the partition wall, as well as those measured by Arts et al.[7] who, however, tested a channel having an aspect ratio equal to 2. They are also different from the ones measured by Ekkad and Han[11] for testing conditions much similar to the present ones ; e. g., in ref. (11) the second high *Nu* region appears quite far downstream of the second outer corner.

Fig. 5 shows the segment-by-segment distribution of the average Nusselt number on each segment normalized by means of Nu^*. Each segment is $0.5D$ long. The diagram on the left hand refers to heating from only one side wall while the diagram on the right hand is relative to heating from both sides. It is possible to notice that up to segment 7 the behaviour of a fully developed flow is practically recovered. However, data relative to the one side heating case shows a slightly higher heat transfer coefficient as it should.

In all diagrams, the average *Nu* continuously increases downstream of segment 7 up to segment 12 (at the entrance of the turn), drops in segment 13 (at the entrance of the outlet duct), increases a little in the two following segments and afterwards continuously decreases towards the value corresponding to a redeveloped flow. For the same heating condition, the *Nu* rise in the turning zone increases as the Reynolds number decreases. For the same Reynolds number, the same increase is higher in the case of heating from both side walls.

Conclusions

Results for the 180deg turn show that the Nusselt number, ahead of the turn, practically coincides with that based on the Dittus-Boelter correlation Nu^*. Across the turn a large increase in *Nu* occurs followed by a subsequent progressive decrease further downstream. Some very high heat transfer coefficient regions are present at the wall; the first one is located on the end wall practically in front of the duct which enters the turn slightly moved towards the partition wall axis; the second region, which exhibits the highest values of Nusselt number is just downstream of the second outer corner; the last one is near the partition wall about two diameters downstream of the second inner corner. Just before the first and second outer corners and attached to the external wall, two recirculation zones to appear at the centre of which the Nusselt number attains a local minimum; but this minimum is always much higher than the corresponding value of Nu^*. Another region of lower *Nu* is attached to the tip of the partition wall, slipping downstream, but *Nu* values also in this case are higher than the corresponding Nu^* ones.

References

1. FAN, C.S. and METZGER, D.E., Effects of Channel Aspect Ratio on Heat Transfer in Rectangular Passages with Sharp 180-Deg Turns, 1987, ASME Paper No. 87-GT-113.
2. METZGER, D.E. and SAHM, M.K., Heat Transfer Around Sharp 180-Deg Turns in Smooth Rectangular Channels, J. Heat Transfer, 1986, Vol. 108, pp. 500-506.
3. CHYU, M.K., Regional Heat Transfer in Two-Pass and Three-Pass Passages with 180-Deg Sharp Turns, J. Heat Transfer , 1991, Vol. 113, pp. 63-70.
4. HAN, J.C., CHANDRA, P.R. and Lau, S.C., Local Heat/Mass Transfer Distributions Around Sharp 180-Deg Turns in Two-Pass Smooth and Rib-Roughened Channel, J. Heat Transfer, 1988, Vol. 110, pp. 91-98.
5. CHANDRA, P.R., HAN, J.C. and LAU, S.C., Effect of Rib Angle on Local Heat/Mass Transfer Distribution in a Two Pass Rib Roughened Channel, J. Turbomachinery, 1988, Vol. 110, pp. 223-241.
6. WANG, T.S. and CHYU, M.K., Influence of Turning Geometry on Convective Transport in Square Duct with a 180-degree Sharp Turn, Proc. Int. Symp. on Heat Transfer in Turbomachinery, Athens, 1992, pp. 1-15.
7. ARTS, T., LAMBERT DE ROUVROIT, M., RAU, G. and ACTON, P., Aero-Thermal Investigation of the Flow Developing in a 180 Degree Turn Channel, Proc. Int. Symp. on Heat Transfer in Turbomachinery, Athens, 1992, Paper N. 10, pp. 1-12.
8. LAU, S.C., RUSSELL, L.M., THURMAN, D.R. and HIPPENSTEELE, S.A., Visualization of Local Heat Transfer in Serpentine Channels with Liquid Chrystals, Proc. V Int. Symp. on Transport Phenomena and Dynamics of Rotating Machinery, Kaanapaly , 1994, Vol. A, pp. 411-423.
9. ASTARITA, T., CARDONE , G. and CARLOMAGNO, G.M., "Heat Transfer and Surface Flow Visualization Around a 180deg Turn in a Rectangular Channel" in Heat Transfer in Turbulent Flows, 1995, Anand N.K. et al. Eds., ASME HTD - Vol. 318, pp. 161-168.
10. CARDONE, G., ASTARITA, T. and CARLOMAGNO, G.M., " Surface Flow Visualization Around a 180deg Turn Channel for Different Aspect Ratios" in Flow Visualization VII, 1995, Crowder J. ed., Begell House, New York, pp. 977-982.
11. EKKAD, S.V. and HAN, J.C., Local Heat Transfer Measurements Near a Sharp 180° Turn of a Two-pass Smooth Square Channel with a Transient Liquid Crystal Image Technique, Proc. V Int. Symp. on Transport Phenomena and Dynamics of Rotating Machinery, Kaanapaly, 1994, Vol. A, pp. 701-716.
12. CARLOMAGNO, G.M., DE LUCA, L., Infrared Thermography in Heat Transfer, in Handbook of Flow Visualization, 1989, Yang W.J. ed., pp. 551-553.